Global entanglement and quantum phase transitions in the transverse XY Heisenberg chain

Roya Radgohar and Afshin Montakhab*
Department of Physics, College of Sciences, Shiraz University, Shiraz 71946-84795, Iran

(Received 5 January 2018; revised manuscript received 15 January 2018; published 30 January 2018)

We provide a study of various quantum phase transitions occurring in the XY Heisenberg chain in a transverse magnetic field using the Meyer-Wallach (MW) measure of (global) entanglement. Such a measure, while being readily evaluated, is a multipartite measure of entanglement as opposed to more commonly used bipartite measures. Consequently, we obtain analytic expression of the measure for finite-size systems and show that it can be used to obtain critical exponents via finite-size scaling with great accuracy for the Ising universality class. We also calculate an analytic expression for the isotropic (XX) model and show that global entanglement can precisely identify the level-crossing points. The critical exponent for the isotropic transition is obtained exactly from an analytic expression for global entanglement in the thermodynamic limit. Next, the general behavior of the measure is calculated in the thermodynamic limit considering the important role of symmetries for this limit. The so-called oscillatory transition in the ferromagnetic regime can only be characterized by the thermodynamic limit where global entanglement is shown to be zero on the transition curve. Finally, the anisotropic transition is explored where it is shown that global entanglement exhibits an interesting behavior in the finite-size limit. In the thermodynamic limit, we show that global entanglement shows a cusp singularity across the Ising and anisotropic transition, while showing non-analytic behavior at the XX multicritical point. It is concluded that global entanglement, despite its relative simplicity, can be used to identify all the rich structure of the ground-state Heisenberg chain.

DOI: 10.1103/PhysRevB.97.024434

I. INTRODUCTION

Quantum phase transition (QPT) occurs as a result of a sudden change in the ground state as a system's parameter (e.g., external field) is slowly changed [1]. Quantum fluctuations, instead of thermal fluctuations, drive such transitions, i.e., $T \approx 0$. This sudden change is accompanied by interesting behavior on the macroscopic level. QPT has attracted intense attention in the field of condensed-matter physics. The prominent examples are quantum Hall systems [2], superconductor-insulator transitions [3], and heavy-fermion compounds [4]. It is not unexpected that such interesting quantum systems should be able to be characterized using tools of quantum information theory [5]. In fact, in recent years, various entanglement measures have been used to study various properties of QPT in strongly interacting quantum systems. This type of approach is interesting because it uses a pure quantum mechanical measure in order to identify and study QPT. Furthermore, since entanglement can be used as a resource for quantum technology, QPT can provide a fertile playground as criticality implies highly correlated systems, which implies maximal entanglement.

Entanglement as an indicator of QPT was initially investigated in Ref. [6], where concurrence as a bipartite entanglement measure was used to extract correlation length exponent in the transverse XY model using a finite-size scaling method. Wei *et al.* [7], on the other hand, used a mulitipartite entanglement measure based on the maximum overlap of a given state with an unentangled state and explicitly extracted the correlation length exponent for Ising transition in XY and XX models as well as detected the classical transition line over which the entanglement measure was shown to be zero. The authors in Ref. [8] have used an entanglement measure obtained by taking an average over entanglement between various bipartite divisions of the isotropic XY chain to detect level crossing points. The standard deviation of these bipartite entanglements determines how many moments must be calculated to get the proper precision. Moreover, concurrence has been used as a measure that is able to detect the anisotropic phase transition in the transverse XY model as it is shown to be maximum at the corresponding critical point for finite-size systems [9].

There are many studies which use various measures (or witnesses) of entanglement (or quantum correlations) in order to identify and characterize quantum critical points. Most such studies consider the more common bipartite measures, which do not seem appropriate for many-body, highly correlated systems. On the other hand, more appropriate multipartite measures are usually difficult to define and and/or to calculate. In this work, we propose to study various QPTs in the XY chain using a multipartite measure which is both simple to define and easy to study. Furthermore, we apply this simple measure to all critical aspects of the XY chain, instead of focusing on a particular transition in the model.

Entanglement as a function of control parameter, its scaling, and its nonanalytic behavior are key issues when studying quantum critical phenomena. While early studies focused on bipartite measures of entanglement [6,10–12], it has recently been argued that a better characterization is provided by multipartite measures of entanglement [7,13]. This is particularly important since criticality is achieved by long-range correlations in short-range interacting systems. Such long-

*montakhab@shirazu.ac.ir

range correlations are argued to be much better characterized by global measures. We therefore propose to study the archetypical XY Heisenberg chain of a spin-1/2 model using the Meyer-Wallach [14] measure of global entanglement. The XY chain in the presence of transverse field plays a central role in condensed matter theory (e.g., quantum Hall effect [15]) and is a good candidate to connect small quantum processors in quantum computers [16] and to transmit information between long-distance sites in quantum communication protocols [17,18].

While being relatively simple, the model exhibits a rich phase diagram, including a quantum Ising critical transition line, an anisotropic transition line, and the intersection of these two lines which provides a unique (XX) multicritical point. The model also exhibits a (classical) transition in the ferromagnetic regime known as the oscillating transition. Most studies have focused on the Ising critical line which belongs to Ising universality class. Here, taking advantage of analytic solutions of the model, we provide expressions for global entanglement. We study all the above transitions using the finite-size limit as well as the infinite-size (thermodynamic) limit. We show that global entanglement is capable of providing important characterizations for each transition considered, including scaling behavior, level crossing, and critical exponents. Our results provide further evidence that a multipartite measure of entanglement could act as a thermodynamic parameter in quantum many-body systems.

The paper is organized as follows: In the next section, we discuss the XY model and its phase diagram. We also provide a brief introduction to global entanglement measure which we use throughout our study. In Sec. III, we first provide an analytical expression of global entanglement for the XY model and extract the correlation length exponent by applying finite-size scaling for the Ising transition. We then calculate the measure for the XX model, determining the level-crossing points as well as obtaining the critical exponent. Next, global entanglement behavior in the thermodynamic limit and the (classical) oscillating line are considered in Sec. IV. In Sec. V, we consider the behavior of global entanglement near the anisotropic phase transition line. We close by summarizing our results and providing some commentary.

II. MODEL AND MEASURE

The system under consideration is a family of models consisting of N spin-1/2 (qubits) arranged in a chain interacting through nearest-neighbor coupling and transverse external field in the z direction. The Hamiltonian of the system is given by

$$H = \sum_{i=0}^{N-1} -J\left(\frac{1+r}{2}\sigma_i^x\sigma_{i+1}^x + \frac{1-r}{2}\sigma_i^y\sigma_{i+1}^y\right) - h\sigma_i^z, \quad (1)$$

where $\sigma_i^\mu (\mu = x,y,z)$ are the Pauli matrices, J is the exchange coupling ($J = 1$ in this paper), h is the strength of the magnetic field, and r measures anisotropy degree of spin-spin interactions in the x-y plane which typically varies from 0 (isotropic model) to 1 (Ising model). Moreover, we impose periodic boundary conditions (PBC) $\sigma_N^x = \sigma_0^x$ and $\sigma_N^y = \sigma_0^y$. This model describes one of the few exactly solvable quantum many-body systems, and its various thermodynamic properties have been extensively investigated in the literature dating back to 1961. The free-field Hamiltonian was originally introduced by Lieb *et al.* in a seminal paper [19]. In the paper, the authors diagonalized XY Hamiltonian by exploiting the Jordan-Wigner transformation and mapping spin-1/2 systems into spinless fermions, and exactly calculated its spectrum and eigenstates as well as the instantaneous correlation functions. Niemeijer [20] added a constant transverse magnetic field to the XY Hamiltonian and calculated the z magnetization in an arbitrary field and temperature as well as z-correlation functions. He also investigated the effect of a small oscillating field superimposed on the constant field and approximately found the time evolution of the magnetization in Ref. [21]. Pfeuty [22] considered a special case of the XY model as $r = 1$, Ising model, with constant transverse field and calculated correlation functions in x,y, and z directions as well as the x and z components of magnetization. In a series of papers, McCoy and his coworkers have intensively investigated the nonequilibrium properties of XY model in the presence of a time-dependent magnetic field in Refs. [23,24] and calculated correlation functions in the case of constant field in Refs. [25,26].

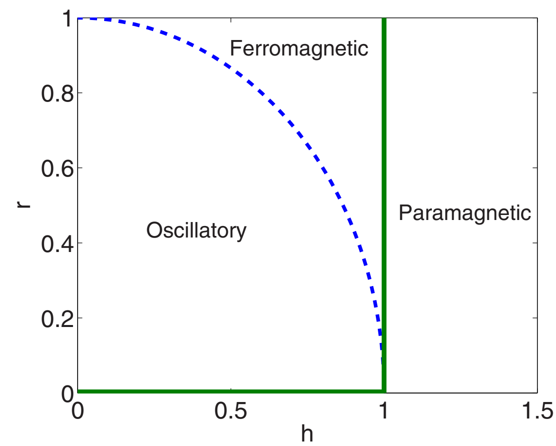

FIG. 1. Phase diagram of the one-dimensional (1D) XY model. Green solid lines $h = 1$ (Ising) and $r = 0$ (anisotropic) are critical lines, and their intersection is the multicritical point. Blue dashed curve separates the oscillatory part of the ferromagnetic phase.

The zero-temperature phase diagram of the model is schematically shown in Fig. 1. In a free-field XY chain ($h = 0$), the system exhibits ferromagnetic order with nonzero magnetization originating from the exchange coupling between nearest-neighbor spins. Adding the external field tends to align the spins in the z direction such that the system undergoes a ferromagnet to paramagnet transition at $h = 1$. The green solid line $h = 1$ represents the (Ising) critical points separating the regimes of ferromagnetic and paramagnetic phase. The other critical green solid line $r = 0$ (isotropic model) is the boundary between the ferromagnetic phases in the x phase (upper half-plane) and y phase (lower half-plane). The intersection of these two lines ($r = 0$ and $h = 1$) is the XX critical point with a different universality class from that of Ising universality. The ferromagnetic phase is divided into two parts by the dashed blue circle: Outside the circle, the correlation functions decay exponentially, while they have oscillatory tails inside

[23]. The ground state on the dashed blue circle (called the classical line) has a simple direct product form of single-qubit states, implying zero two-point functions and extremely short correlation length [27].

Quite generally, correlations are expected to reach a maximum as long-range correlations dominate system's behavior at the critical point. QPT occurs when small variation in the parameters of Hamiltonian fundamentally changes the symmetry of the ground state, resulting in the actual level crossing or the limiting case of avoided level crossing between the ground and excited state [1]. At the critical point, the length scale characterizing the exponential decay or the crossover of correlation functions diverges as $\xi \sim |h - h_c|^{-\nu}$. On the other hand, entanglement, as a purely quantum mechanical property, has a close relation with quantum correlations and can be exploited as an indicator of quantum phase transition [6,7]. However, bipartite measures of entanglement between individual qubits typically decay fast as a function of distance even near the critical point [6,10–12]. It is therefore expected that a more global (multipartite) measure of entanglement would provide a more appropriate measure to study criticality in QPT.

In this paper, we use global entanglement measure introduced by Meyer and Wallach [14]. The measure is a function of N-qubit pure states of $|\psi\rangle \in (\mathbb{C}^2)^{\otimes N}$ as

$$E_g(|\psi\rangle) = \frac{4}{N}\sum_{k=1}^{N} D(|\tilde{u}^k\rangle,|\tilde{v}^k\rangle), \tag{2}$$

where the non-normalized vectors $|\tilde{u}^k\rangle$ and $|\tilde{v}^k\rangle$ are the projections of the state $|\psi\rangle$ onto the kth-qubit subspaces

$$|\psi\rangle = |0\rangle \otimes |\tilde{u}^k\rangle + |1\rangle \otimes |\tilde{v}^k\rangle \tag{3}$$

and D is the norm squared of the wedge product of two vectors $|\tilde{u}^k\rangle$ and $|\tilde{v}^k\rangle$ as

$$D(|\tilde{u}^k\rangle,|\tilde{v}^k\rangle) = \sum_{i<j} \left|\tilde{u}_i^k \tilde{v}_j^k - \tilde{u}_j^k \tilde{v}_i^k\right|^2. \tag{4}$$

Meyer and Wallach [14] proved that this measure is entanglement monotone in the sense that it is a nonincreasing function under local operations and classical communications (LOCC). Using the invariance under local operations, $|\psi\rangle$ can be written in the Schmidt basis over bipartite divisions of the kth qubit and other qubits, that simplifies Eq. (2) as [28]

$$E_g = 2\left[1 - \frac{1}{N}\sum_{k=0}^{N-1} \mathrm{tr}\left(\rho_k^2\right)\right], \tag{5}$$

where ρ_k is the reduced density matrix for the kth qubit obtained by tracing over other qubits. Global entanglement (E_g) has been used to detect quantum critical points [29], and its scaling properties for the Ising model in various dimensions have been studied in Ref. [13]. It has also been used to study decoherence effects in finite-qubit systems [30].

Since the MW measure was unable to distinguish global and subglobal entanglements (e.g., globally entangled four-qubit state and product of two two-qubit entangled states [31]), Scott [32] generalized the MW measure to multiqudit states of $|\psi\rangle \in (\mathbb{C}^D)^{\otimes N}$ considering all the possible bipartite divisions as

$$Q_m(\psi) = \frac{D^m}{D^m - 1}\left[1 - \frac{m!(N-m)!}{N!}\sum_{|S|=m} \mathrm{tr}\left(\rho_S^2\right)\right] \tag{6}$$

in which $m = 1,2,\ldots,[N/2]$ ($[k]$ denotes the integer part of k) and S is a set of m qubits. Although Q_m is able to distinguish between fully global and subglobal entanglements, its direct computation is a quite challenging task for realistic models as it requires all m-site reduced-density matrices. We therefore propose to study the XY model using E_g to see how much information one can extract regarding various transitions using such a measure.

III. ISING QUANTUM PHASE TRANSITION

A. XY model

The transverse XY Heisenberg model has been solved in Ref. [19] by the Jordan-Wigner transformation which maps the spin operators σ_i into the spinless fermionic operators:

$$\sigma_i^z = 1 - 2c_i^\dagger c_i, \qquad \sigma_i^\dagger = \left(\Pi_{j<i}\sigma_j^z\right)c_i, \tag{7}$$

followed by Fourier transformation

$$c_k = \frac{1}{\sqrt{N}}\sum_{j=0}^{N-1} \exp\left(-\frac{2\pi i k j}{N}\right)c_j \tag{8}$$

and Bogoliubov transformation

$$b_k = c_k \cos(\theta_k/2) - i c_{-k}^\dagger \sin(\theta_k/2), \tag{9}$$

where $\cos\theta_k = \frac{\cos(2\pi k/N) - h}{\omega_k}$ and

$$\omega_k = \sqrt{[h - \cos(2\pi k/N)]^2 + r^2\sin^2(2\pi k/N)} \tag{10}$$

are obtained in Ref. [23]. Thus, the Hamiltonian takes the diagonal form

$$H = \sum_k \omega_k (b_k^\dagger b_k - 1), \tag{11}$$

where we may neglect the boundary terms for large systems. We want to obtain an analytical expression for global entanglement of the XY chain in the presence of a traverse magnetic field. To this end, we expand the reduced density matrix ρ_i as [33]

$$\rho_i = \frac{1}{2}\left(q_0 I + \sum_{\mu=x,y,z} q_\mu \sigma_i^\mu\right), \tag{12}$$

where I is the identity matrix and $\sigma_i^\mu (\mu = x,y,z)$ are the Pauli matrices at the ith qubit. The reality of the Hamiltonian [Eq. (1)] and its global phase-flip symmetry ($[\Pi_{i=0}^{N-1}\sigma_i^z, H] = 0$) implies $q_x = q_y = 0$. In addition, the reduced density matrix is unit trace, so $q_0 = 1$, and the single-particle density matrix can be written as [33]

$$\rho_i = \tfrac{1}{2}\left(I + \langle\sigma_i^z\rangle\sigma_i^z\right), \tag{13}$$

where [23]

$$\langle\sigma_i^z\rangle = -\frac{2}{N}\sum_{k=1}^{\frac{N-1}{2}} \frac{\cos(2\pi k/N) - h}{\sqrt{r^2\sin^2\left(\frac{2\pi k}{N}\right) + \left[h - \cos\left(\frac{2\pi k}{N}\right)\right]^2}} - \frac{1}{N} \tag{14}$$

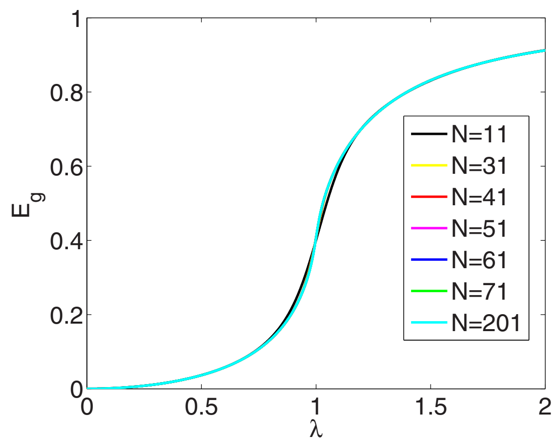

FIG. 2. Global entanglement for a transverse XY chain ($r = 0.5$) as a function of Hamiltonian parameter $\lambda = J/h$ for various system sizes.

and we consider odd number of qubits. Since we use PBC, the single-particle density matrix is the same for all the qubits of chain, and using Eq. (5) we get [13]

$$E_g = 2\left(1 - \mathrm{tr}\rho_i^2\right). \tag{15}$$

The global entanglement in this case can be obtained as

$$E_g = 1 - \langle\sigma_i^z\rangle^2. \tag{16}$$

We begin our analysis by considering E_g as a function of $\lambda = \frac{J}{h}$ for various system sizes N and fixed value of $r = 0.5$. The results are shown in Fig. 2. E_g increases from zero at $\lambda = 0$ ($h \to \infty$), where the ground state of the system is a product state of spins aligned in the z direction and reaches its maximal value $E_g = 1$ with a sharp rise at (the finite-size) transition point, λ_m. A better picture arises when one looks at the derivative of such a function, which displays a divergence at the critical point in the thermodynamic limit. Figure 3 displays such information. As the system size grows, the peak of the derivative approaches the critical point as it diverges in its value. As indicated in the inset, the divergence is logarithmic, indicating a slow divergence. However, the convergence to the critical point is fast as λ_m approaches the critical point $\lambda_c = 1$ with $|\lambda_m - \lambda_c| \sim N^{-\alpha}$ with relatively large "finite-size exponent" of $\alpha = 3.34$. As indicated in the inset, the maximum value of the derivative $dE_g/d\lambda$ obeys

$$\frac{dE_g}{d\lambda}\Big|_{\lambda_m} \approx \kappa_1 \ln N \tag{17}$$

with $\kappa_1 = 0.9783$.

We next calculate the all-important critical exponent ν using finite-size scaling of the derivative of E_g. The scaling relation we use is $\frac{dE_g}{d\lambda} \sim Q[N^{1/\nu}(\lambda - \lambda_m)]$ with $Q(x) \sim ln(x)$ [34]. As can be seen in Fig. 4, all the curves of $F = 1 - \exp[\frac{dE_g}{d\lambda} - \frac{dE_g}{d\lambda}|_{\lambda=\lambda_m}]$ as a function of $N^{1/\nu}(\lambda - \lambda_m)$ collapse nicely on a single curve for $\nu = 1$, in agreement with the well-known result for the Ising universality class [25]. We finally note that our results were obtained for $r = 0.5$; however, similar results hold for $0 < r \leqslant 1$.

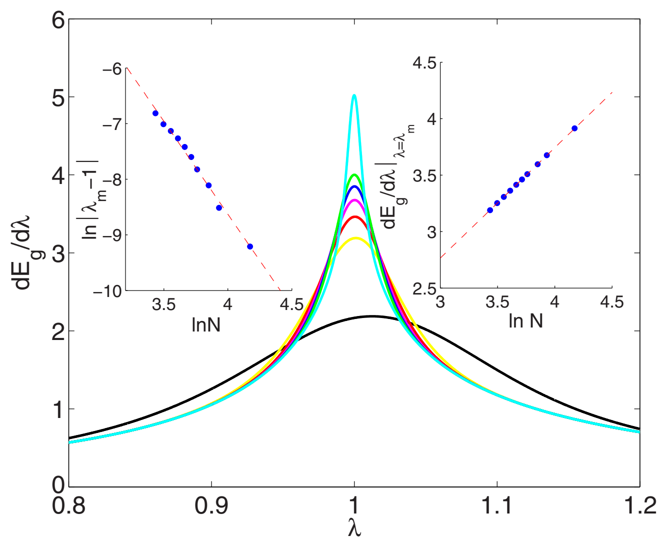

FIG. 3. The derivative of global entanglement for a transverse XY chain ($r = 0.5$) as a function of Hamiltonian parameter λ for various system sizes. The left inset shows that the maximal value λ_m approaching the critical point $\lambda_c = 1$ as $|\lambda_m - \lambda_c| \sim N^{-3.34}$. The right inset shows the logarithmic divergence of the peak as a function of N, $\frac{dE_g}{d\lambda}|_{\lambda_m} \approx \kappa_1 \ln N$, where $\kappa_1 = 0.9783$. The system sizes are the same as in Fig. 2.

B. XX model

The XX model is the isotropic case of the XY Heisenberg model which belongs to a different universality class from that of the Ising. In this model, as the magnetic field is varied, the energy gap between the ground and the first excited state vanishes and the intersections exhibit a sequence of level-crossing points for the finite-size chains. Since the global entanglement directly depends on the ground state of the system, we expect to see sudden jumps in E_g at the level-crossing points. To this end, we are interested in the global entanglement behavior for finite-size chains where the boundary effect terms of the Hamiltonian cannot be neglected. These terms break the periodicity of the Jordan-Wigner operators

$$c_i^\dagger = \left(\Pi_{j<i}\sigma_j^z\right)\sigma_i^\dagger = e^{i\pi n_i \downarrow}\sigma_i^\dagger \tag{18}$$

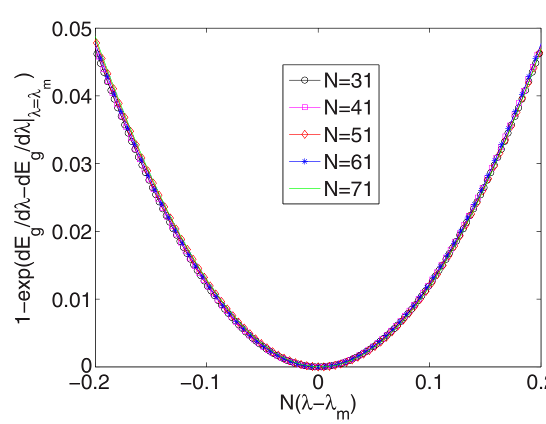

FIG. 4. Finite-size-scaling data collapse of derivative of global entanglement for transverse XY chain ($r = 0.5$). The best collapse of $\frac{dE_g}{d\lambda} \sim Q[N^{1/\nu}(\lambda - \lambda_m)]$ occurs at $\nu = 1$.

as

$$c_0^\dagger = \sigma_0^\dagger, \qquad c_N^\dagger = e^{i\pi n_{N\downarrow}}\sigma_N^\dagger = e^{i\pi n_{N\downarrow}}\sigma_0^\dagger, \tag{19}$$

in which $n_{i\downarrow}$ is the operator counting the total number of down spins in the chain. In this case, the Hamiltonian can be diagonalized by the Jordan-Wigner transformation and the following deformed Fourier transformation [8]:

$$c_j = \frac{1}{\sqrt{N}} e^{\frac{2\pi i \alpha_j}{N}} \sum_k e^{-ikj} c_k, \tag{20}$$

where α_j is a local gauge. The ground state of this model was obtained in Ref. [8] as

$$|\psi_n\rangle = \frac{1}{\sqrt{N}} \sum_{j_1<j_2<\ldots<j_n} \{\lambda_{j_1,j_2,\ldots,j_n}(-1)^{nj_1}(-1)^{(n-1)(j_2-j_1)} (-1)^{(n-2)(j_3-j_2)}\ldots(-1)^{j_n-j_{n-1}}\}|\downarrow\rangle_0\ldots|\uparrow\rangle_{j_1}\ldots|\uparrow\rangle_{j_2} \ldots|\uparrow\rangle_{j_n}\ldots|\downarrow\rangle_{N-1}, \tag{21}$$

while $\lambda_{j_1,j_2,\ldots,j_n}$ is given by

$$\lambda_{j_1,j_2,\ldots,j_n} = \sum_p (-1)^p \exp\left[\frac{2\pi i}{N}(k_1 j_{p_1} + k_2 j_{p_2} + \cdots + k_n j_{p_n})\right] \tag{22}$$

and $1 \leqslant n \leqslant [N/2]$ depends on the magnetic field h such that

$$\frac{\sin\left[\frac{(n+1)\pi}{N}\right] - \sin\left(\frac{n\pi}{N}\right)}{\sin(\pi/N)} < h \leqslant \frac{\sin\left(\frac{n\pi}{N}\right) - \sin\left[\frac{(n-1)\pi}{N}\right]}{\sin(\pi/N)}. \tag{23}$$

Moreover, the sum [in Eq. (22)] extends over the permutation group. Therefore, the z magnetization is $\langle\sigma_i^z\rangle = 1 - \frac{2n}{N}$. This allows us to calculate global entanglement in an analytic fashion for finite size system, which leads to

$$E_g = \frac{4n(N-n)}{N^2}. \tag{24}$$

Interestingly, this indicates a steplike behavior for the E_g as a function of h. In fact, the points $h_s = \frac{\sin(\frac{n\pi}{N}) - \sin[\frac{(n-1)\pi}{N}]}{\sin(\pi/N)}$ are exactly the same as the level-crossing points obtained by the exact solution of XX model; see Ref. [8]. Figure 5 shows the global entanglement for an XX chain of $N = 15$ qubits obtained from Eq. (24) in terms of h. The stepwise behavior of global entanglement determines the position and number of level crossings in the system. Note that the number of steps is $[N/2]$.

It might be interesting to look into the behavior of E_g in the thermodynamic limit for the XX model to see what happens to the steplike structure, as well as the behavior near the critical point. In the thermodynamics limit, we can neglect the boundary effects, use Eq. (14) at $r = 0$, and write the global entanglement for XX model

$$E_g = 1 - \left\{\frac{1}{\pi}\int_0^\pi \frac{h - \cos(\phi)}{|h - \cos(\phi)|}\right\}^2 = 1 - \frac{1}{\pi^2}(2\phi_c - \pi)^2, \tag{25}$$

where $\phi_c = \cos^{-1}(h)$ is the pole of the denominator. The behavior is shown as an inset in Fig. 5. The effect of finite number of steps naturally disappear and E_g behaves much as

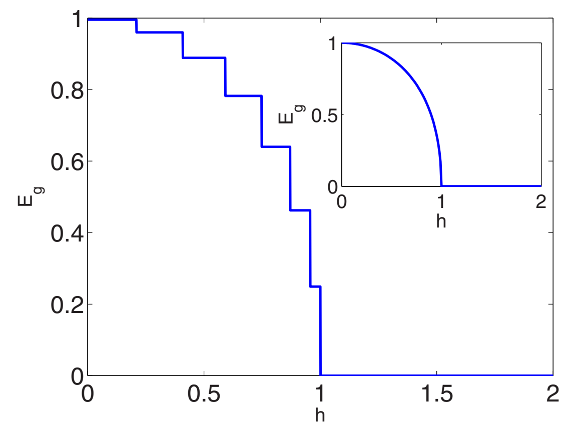

FIG. 5. Global entanglement [Eq. (24)] as a function of magnetic field for XX Heisenberg ($r = 0$) chain of $N = 15$ qubits. The level crossings coincide with jumps in E_g. The inset shows the $N \to \infty$ limit.

an order parameter for this transition. One can also use this expression to obtain scaling of the derivative of entanglement in order to obtain correlation length exponent [7,35]. Hence, we get

$$\frac{dE_g}{dh}|_{h\to 1^-} \approx \frac{4\sqrt{2}}{\pi^2}\frac{1}{\sqrt{1-h}}. \tag{26}$$

This allows us to obtain the exponent ν, which governs the divergence of the correlation length as $\frac{dE_g}{dh} \sim |h-1|^{-\nu}$ with $\nu = 1/2$, consistent with previous reports [25].

IV. THERMODYNAMIC LIMIT AND THE CLASSICAL LINE

In the previous section, we used the finite-size behavior of E_g in order the characterize the behavior of QPT at $h = 1$, as well as characterizing the XX model. We also obtained a closed form expression for E_g in the thermodynamics limit which allowed us to calculate the critical exponent for this universality class. We now propose to calculate E_g in the thermodynamic limit for the entire parameter regime and extract more information in this limit of the system, paying particular attention to the so-called classical transition. Let us start by explaining the simplest model of XY Heisenberg family, the Ising model ($r = 1$). In the absence of external field ($h = 0$), the spins are either all pointed in the positive or negative x direction and the corresponding ground state is doubly degenerate. Turning on a small h may be regarded as a perturbation changing the orientation of a small fraction of spins to the opposite direction. In the case of a finite-size system, such a field induces quantum tunneling between the degenerate ordered states and leaves the system in a superposition state satisfying phase-flip symmetry. As we go to the thermodynamic limit, this energy barrier becomes infinitely high such that it does not allow tunneling events for any finite h and therefore keeps the system in the degenerate ground state [36]. Therefore, this breaking of phase-flip symmetry requires us to take into account the coefficient q_x in Eq. (12) and rewrite Eq. (13) as [33]

$$\rho_i = \tfrac{1}{2}\left(I + \langle\sigma_i^z\rangle\sigma_i^z + \langle\sigma_i^x\rangle\sigma_i^x\right), \tag{27}$$

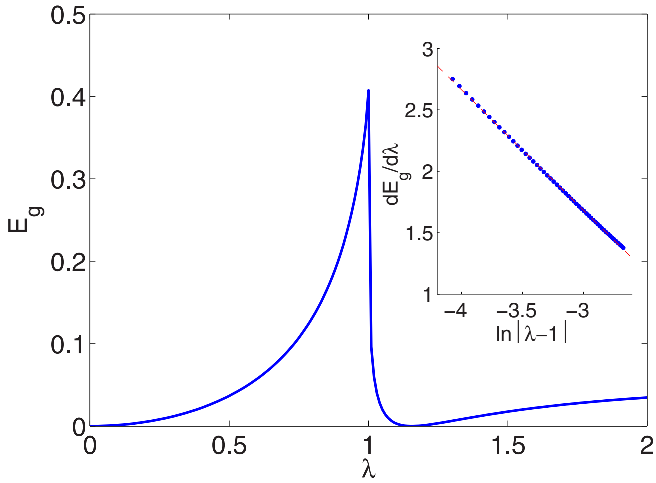

FIG. 6. Global entanglement as a function of λ for $r = 0.5$ in the thermodynamic limit. The inset displays the logarithmic divergence behavior of $dE_g/d\lambda$ as it approaches the critical point. The slope gives $\kappa_2 = -0.9789$.

where [23]

$$\langle \sigma^z \rangle = \frac{1}{\pi} \int_0^{\pi} d\phi \frac{h - \cos(\phi)}{\sqrt{r^2 \sin^2(\phi) + [h - \cos(\phi)]^2}} \tag{28}$$

and [25]

$$\langle \sigma^x \rangle = \begin{cases} 2[2(1+r)]^{-1/2} r^{1/4} (1-h^2)^{1/8} & \text{if } h \leqslant 1 \\ 0 & \text{otherwise} \end{cases}. \tag{29}$$

Given the above and considering Eq. (15), global entanglement can now be obtained for the entire parameter regime in the thermodynamic limit. Figure 6 shows an example for E_g as a function of λ for $r = 0.5$.

In the weak exchange regime ($\lambda < 1$), the XY Hamiltonian term may be regarded as a perturbation that is unable to break the phase-flip symmetry and therefore leaves the system in a nondegenerate ground state, so E_g in this case is the same as the one for finite-size chains (see Fig. 2). At the critical point, $\langle \sigma^x \rangle$ begins to rise, breaking the phase-flip symmetry, leading to a sudden decline in entanglement, and exhibiting absolute maximal value for entanglement at the critical point. This, by the way, is consistent with the general expectation of highly correlated system at the critical point [29,33]. However, entanglement quickly decreases and vanishes at $\lambda = 1.15$ ($h = 0.87$) where the ground state is unentangled (product states) since it lies exactly on the classical line $r^2 + h^2 = 1$. In order to obtain a better understanding of the behavior of E_g, we plot it in terms of h and r in Fig. 7.

For all the nonzero anisotropic parameter, E_g is maximum on the Ising transition line separating paramagnetic and ferromagnetic phases. In the case of $r = 0$ (isotropic model), the global entanglement exhibits a different behavior indicating a different universality class. For a better understanding, a corresponding contour plot is provided in Fig. 8.

Here, we can more clearly see the behavior on the classical line. The solid black line separates the oscillation part of ferromagnetic phase in the diagram phase where the ground state is a product state and E_g is exactly zero along this

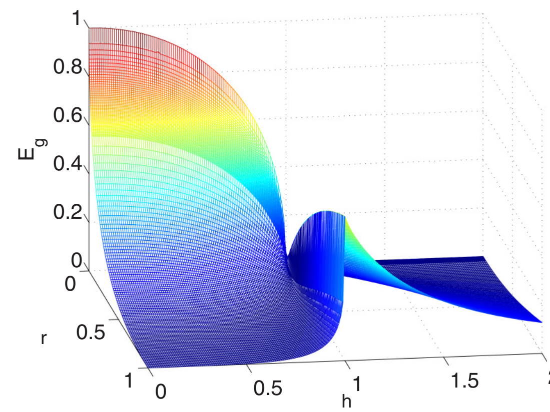

FIG. 7. Three-dimensional (3D) plot of global entanglement as a function of r and h in the thermodynamic limit.

transition. Therefore, E_g is also able to indicate the transition to the oscillating phase in the ferromagnetic case as it becomes zero across such transition. We note that this value of zero, and therefore indicator of the classical transition, is only valid in the thermodynamic limit and does not occur for the finite-size systems. Note also that in the thermodynamic limit entanglement is maximal at the critical point as expected but only exhibits a sharp (well-behaved) rise for the finite N even if N is taken to be very large. This provides a good indication that E_g can behave similarly to the usual thermodynamic functions, as they *only* exhibit *nonanalytic* behavior (at criticality) in the thermodynamic limit; compare Fig. 2 with Fig. 6. Moreover, the inset in Fig. 6 shows that the derivative of global entanglement $dE_g/d\lambda$ for an infinite chain diverges as

$$\frac{dE_g}{d\lambda} \approx \kappa_2 \ln|\lambda - 1|, \tag{30}$$

where $\kappa_2 = -0.9789$. Based on the scaling ansatz for logarithmic divergence [34], the ratio of $|\kappa_1/\kappa_2|$ is the correlation length exponent, ν. In our case, this ratio is given by $|\kappa_1/\kappa_2| = 0.994$ which is very close to the exact result $\nu = 1$ as well as our

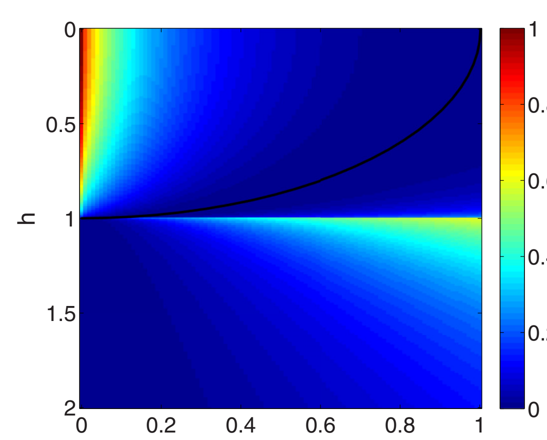

FIG. 8. Contour plot of global entanglement versus the external field and anisotropic parameter.

result in Sec. III A. We also note similar results are obtained using concurrence in Ref. [6] and geometric phase in Ref. [35].

V. ANISOTROPIC QUANTUM PHASE TRANSITION

Another quantum phase transition occurs over the line $r = 0$ for $0 < h < 1$, the anisotropic transition, which has received less attention in the literature [9,37,38]. The anisotropic phase transition separates two ferromagnetic phases with orderings in the x ($r > 0$) and y ($r < 0$) directions and belongs to a different universality class than the Ising class. Figure 9 shows global entanglement as one crosses such a transition for the fixed value of $h = 0.5$.

As can be seen in this figure, there is a distinct change in the global entanglement around $r = 0$, which is the local extremum. However, it may be minimum or maximum, depending on the system size. We have observed that when one is close but below (above) the level crossing point, E_g is convex (concave), slowly changing shape as one crosses a given step for a fixed N. Therefore, the picture that emerges is that for a finite chain, the first derivative of E_g is zero at the anisotropic transition, indicating a local maximum or a minimum depending on whether the given values of h and N places us near the left or right edge of the step. This pattern continues to hold across the anisotropic transition until one gets to the multicritical point ($h = 1, r = 0$), where E_g displays a local minimum approaching zero in the thermodynamic limit; see, for example, Fig. 5. This type of behavior continues to hold for $h > 1$. Note that E_g does not approach zero with increasing N as one crosses the anisotropic transition. Therefore, one can conclude that the finite-size behavior of E_g distinguishes the critical anisotropic transition. However, one would like to know if E_g exhibits any nonanalytic behavior associated with (critical) quantum phase transitions. To investigate this, we need to calculate global entanglement across the anisotropic transition in the thermodynamics limit.

In order to calculate global entanglement for $r < 0$ in the thermodynamic limit, we need to make the following observations. In the regime of positive anisotropic parameter,

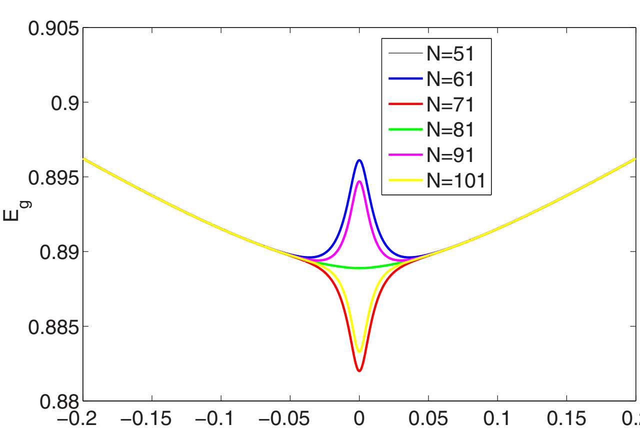

FIG. 9. Global entanglement versus r for the fixed magnetic field ($h = 0.5$) and different system sizes. As N changes, the step structure of the finite XX model changes, leading to the behavior observed.

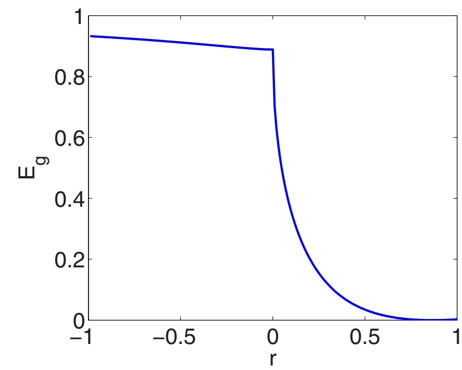

FIG. 10. Global entanglement in terms of r for a fixed value of $h = 0.5$ in thermodynamic limit.

magnetization in the y direction is zero and ρ_i is a function of σ_x and σ_z as shown in Sec. IV, i.e., Eqs. (27), (28), and (29). Therefore, E_g is given by Eq. (15). It is evident from the Hamiltonian that transformation $r \to -r$ interchanges σ_x with σ_y, which leads to the zero value of $\langle\sigma_x\rangle$ for $r < 0$ [19]. Therefore, since the y component of magnetization does not contribute to E_g, due to the reality of Hamiltonian, a single-particle density matrix is given by $\rho_i = \frac{1}{2}(I + \langle\sigma_z\rangle\sigma_z)$, and E_g is given by Eq. (16) in this regime. Therefore, the picture that emerges is that for $h > 1$ where one is in the paramagnetic phase and no phase transition occurs at $r = 0$, E_g is symmetric about this minimum point for a given value of h. However, one expects that the broken symmetry due to $\langle\sigma_x\rangle$ at $r = 0$ and $h < 1$ leads to a broken symmetry of E_g about the transition point. This is indeed the case, as can be seen from Fig. 10, which shows E_g for $h = 0.5$ across the anisotropic transition. Clearly one can see the nonanalytic behavior is similar to thermodynamic quantities at a critical point. We conclude that E_g can distinguish the critical anisotropic transition in the XY model.

VI. CONCLUSIONS

In this paper, we have used the MW measure of global entanglement in order to study various quantum phase transitions occurring in the transverse XY Heisenberg chain. Our main motivation has been the observation that a multipartite measure of entanglement is much better suited for studying QPT than the standard bibipartite measures. However, most multipartite measures are difficult to calculate. We have been able to calculate global entanglement both in the finite-size limit as well as the thermodynamic limit analytically. The finite-size study was shown to be very useful for extracting the critical exponents for the Ising transition, via the derivative of entanglement. In the thermodynamic limit, E_g was shown to exhibit nonanalytic behavior at the Ising transition, while having maximal value. The thermodynamic limit of global entanglement was also used to extract critical exponent for the multicritical point of the XX model. For the finite-size system, the step structure of level crossings was exactly reproduced by global entanglement. Also, while the finite-size measure of global entanglement did not show any particular behavior across the classical oscillating transition, the thermodynamic limit of the measure was able to signal such a transition as it took on vanishing value across this classical transition. Furthermore, we studied the anisotropic transition where global entanglement was shown to exhibit a nonanalytic behavior across such a transition in the thermodynamic limit, while showing an interesting, N-dependent behavior for the finite size case. Therefore, the cusp singularity at both quantum transitions, nonanalyticity at the multicritical point, and vanishing value on the classical curve is the general behavior of global entanglement in the thermodynamic limit. This type of behavior is what one would expect from a genuine (quantum) thermodynamic variable. We therefore conclude that global entanglement, despite its simplicity, can produce much of the rich behavior of the XY model in various parameter regimes, identifying all the transition points. Such a multipartite measure of entanglement seems to be a good candidate for studying the thermodynamic behavior of many-body quantum systems.

We end by making the following observation. We have seen that while finite-size study of entanglement can produce interesting behavior including scaling properties, it was the thermodynamic limit of entanglement which was able to fully bring to light the various transitions in the XY model. In particular, the thermodynamic limit exhibit properties which one would have never seen for finite N, even for very large values of N. This is particularly alarming, as many studies of entanglement and quantum phase transitions are limited by finite-size studies with the belief that numerically exact finite-size solutions can be extrapolated to find the thermodynamic limit.

ACKNOWLEDGMENTS

Support from Shiraz University Research Council is noted. Useful discussions with R. Najafinia and M. Pouranvari in the early phase of this project are also acknowledged.

[1] S. Sachdev, *Quantum Phase Transitions* (Cambridge University Press, Cambridge, UK, 2013).
[2] S. L. Sondhi, S. M. Girvin, J. P. Carini, and D. Shahar, Rev. Mod. Phys. **69**, 315 (1997).
[3] D. B. Haviland, Y. Liu, and A. M. Goldman, Phys. Rev. Lett. **62**, 2180 (1989).
[4] P. Coleman, Phys. B (Amsterdam, Neth.) **259**, 353 (1999).
[5] M. A. Nielsen and I. L. Chaung, *Quantum Information and Quantum Computation* (Cambridge University Press, Cambridge, UK, 2000).
[6] A. Osterloh, L. Amico, G. Falci, and R. Fazio, Nature (London) **416**, 608 (2002).
[7] T. C. Wei, D. Das, S. Mukhopadyay, S. Vishveshwara, and P. M. Goldbart, Phys. Rev. A **71**, 060305 (2005).
[8] A. D. Pasquale, G. Costantini, P. Facchi, G. Florio, S. Pascazio, and K. Yuasa, Eur. Phys. J.: Spec. Top. **160**, 127 (2008).
[9] M. Zhong and P. Tong, J. Phys. A: Math. Theor. **43**, 505302 (2010).
[10] S. Gu, G. Tian, and H. Lin, Chin. Phys. Lett. **24**, 2737 (2007).
[11] S.-J. Gu, H.-Q. Lin, and Y.-Q. Li, Phys. Rev. A **68**, 042330 (2003).
[12] J. Vidal, G. Palacios, and R. Mosseri, Phys. Rev. A **69**, 022107 (2004).
[13] A. Montakhab and A. Asadian, Phys. Rev. A **82**, 062313 (2010).
[14] D. A. Meyer and N. R. Wallach, J. Math. Phys. **43**, 4273 (2002).
[15] U. Schollwöck, J. Richter, D. Farnell, and R. Bishop, *Quantum Magnetism* (Springer-Verlag, Berlin, 2004).
[16] S. B. Zheng and G. C. Guo, Phys. Rev. Lett. **85**, 2392 (2000).
[17] G. Vidal, J. I. Latorre, E. Rico, and A. Kitaev, Phys. Rev. Lett. **90**, 227902 (2003).
[18] S. Bose, Phys. Rev. Lett. **91**, 207901 (2003).
[19] E. Lieb, T. Schultz, and D. Mattis, Ann. Phys. **16**, 407 (1961).
[20] T. Niemeijer, Phys. (Amsterdam, Neth.) **36**, 377 (1967).
[21] T. Niemeijer, Phys. (Amsterdam, Neth.) **39**, 313 (1968).
[22] P. Pfeuty, Ann. Phys. **57**, 79 (1970).
[23] E. Barouch, B. M. McCoy, and M. Dresden. Phys. Rev. A **2**, 1075 (1970).
[24] E. Barouch and B. M. McCoy, Phys. Rev. A **3**, 2137 (1971).
[25] E. Barouch and B. M. McCoy, Phys. Rev. A **3**, 786 (1971).
[26] B. M. McCoy, E. Barouch, and D. B. Abraham, Phys. Rev. A **4**, 2331 (1971).
[27] J. Kurmann, H. Thomas, and G. Müller, Phys. A (Amsterdam, Neth.) **112**, 235 (1982).
[28] G. K. Brennen, Quant. Inf. Comp. **3**, 619 (2003).
[29] T. R. de Oliveira, G. Rigolin, M. C. de Oliveira, and E. Miranda, Phys. Rev. Lett. **97**, 170401 (2006).
[30] A. Montakhab and A. Asadian, Phys. Rev. A **77**, 062322 (2008).
[31] P. J. Love, A. M. Brink, A. Y. Smirnov, M. H. S. Amin, M. Grajcar, E. Il'ichev, A. Izmalkov, and A. M. Zagoskin, Quant. Inf. Process. **6**, 187 (2007).
[32] A. J. Scott, Phys. Rev. A **69**, 052330 (2004).
[33] T. J. Osborne and M. A. Nielsen, Phys. Rev. A **66**, 032110 (2002).
[34] M. N. Barber, in *Phase Transitions and Critical Phenomena* (Academic, London, 1983), Vol. 8, pp. 146–259.
[35] S. L. Zhu, Phys. Rev. Lett. **96**, 077206 (2006).
[36] J. Larson and E. K. Irish, J. Phys. A: Math. Theor. **50**, 174002 (2017).
[37] R. W. Cherng and L. S. Levitov, Phys. Rev. A **73**, 043614 (2006).
[38] M. M. Rams and B. Damski, Phys. Rev. A **84**, 032324 (2011).